Oikos

OIK-01025

Wittmann, M. J., Metzler, D., Gabriel, W. and Jeschke, J. M. 2013. Decomposing propagule pressure: the effects of propagule size and propagule frequency on invasion success. – Oikos 000: 000–000.

Supplementary material

for: Wittmann, M.J., Metzler, D., Gabriel, W. and Jeschke, J. M. 2013. Decomposing propagule pressure: the effects of propagule size and propagule frequency on invasion success. – Oikos 000: 000–000.

Appendix 1 Formal development of hypotheses

To formalize the hypotheses developed in the main text, let us consider the following stochastic process: Some entity, e.g. a population or a vehicle, starts at position 0 and, at rate f, makes jumps of magnitude s. Between jumps, the entity moves with constant velocity v, but only at positions greater than 0 (see Fig. A1 for example trajectories). In analogy to our overall research question, we ask: Is the expected time until the entity reaches some target position R shorter with many small jumps or with fewer large jumps?

To address this question, let N_t be a random variable for the number of jumps during some time interval of length t. Then N_t is Poisson distributed with parameter $f \cdot t$. Further, let $X_t = s \cdot N_t$ be the displacement of the entity due to these jumps. Then

$$\mathbf{E}[X_t] = \mathbf{E}[s \cdot N_t] = s \cdot \mathbf{E}[N_t] = s \cdot f \cdot t \,. \tag{A1}$$

Thus, the average velocity with which the entity moves is $\bar{v} = s \cdot f + v$, and so it depends only on the product of s and f.

If the average velocity is positive, i.e. in easy scenarios, the expected time to reach the target state R should be approximately $R/\bar{v}$. The observed advantage of a high propagule frequency or jump rate f in easy scenarios can be explained by two kinds of edge effects (Fig. A1 a). The first edge effect results from the fact that movement only starts after the

first jump out of position 0. Thus the higher the jump rate is, the earlier the system starts to move deterministically towards its target. To understand the second edge effect, compare the scenario where jumps of magnitude $2s$ occur at rate $f/2$ to the scenario with magnitude s and rate f. Assume that the system is already within distance s of the target state. Then the expected time until the target is reached is $2/f$ in the former scenario, and only $1/f$ in the latter scenario with the higher jump rate. In the former scenario, the system overshoots the target, an effort that can be considered wasted if only the time to reach the target state is of interest. While the first edge effect is particularly strong if the jump rate is small compared to the velocity v, the second becomes important if the distance between start and target position is small.

In contrast, in difficult scenarios with a negative average velocity, our entity of interest would never reach the target state under a deterministic model. In our stochastic model, however, the target state will eventually be reached when the displacement during some time interval t is considerably larger than expected due to a chance accumulation of jumps (Fig. A1 b). A measure of how frequent such unusual events are is the variance of the displacement

$$\mathbf{Var}(X_t) = \mathbf{Var}(s \cdot N_t) = s^2 \cdot \mathbf{Var}(N_t) = s^2 \cdot f \cdot t \,. \tag{A2}$$

Thus for a fixed value of the product $s \cdot f$, the variance increases with the magnitude of jumps s and thus the expected time to reach the target state decreases. The more negative the average growth rate is, the stronger is this effect (see Fig. A2).

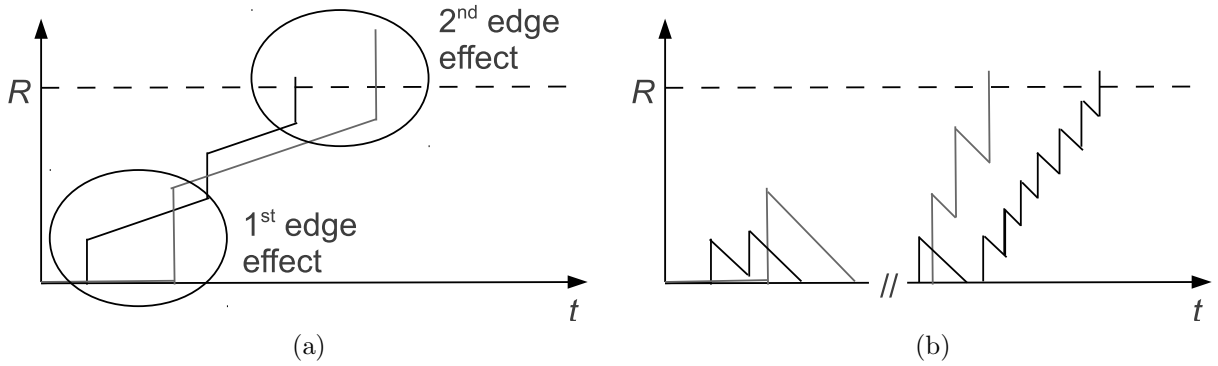

Figure A1. Example trajectories illustrating the heuristic arguments for (a) "easy" ecological scenarios and (b) "difficult" ecological scenarios. The gray lines correspond to introduction regimes with low propagule frequency and high propagule size whereas the black lines represent scenarios with high propagule frequency and low propagule size.

Appendix 2 Details on the Markov processes and their analysis

Single-population model

Each state of this Markov process is characterized by the current population size of the alien species $i \in \{0, 1, 2, \dots\}$. From state i, the system jumps to other states $j \in \{0, 1, 2, \dots\}$ at rates

$$\bar{\lambda}_{i,j} = \begin{cases} b(i) & \text{for } j = i + 1 \\ d(i) & \text{for } j = i - 1 \\ 0 & \text{otherwise} \end{cases}, \tag{A3}$$

where $b(i)$ and $d(i)$ are the rates at which birth and death events, respectively, occur in the population. Transitions due to introduction events happen at rate

$$\hat{\lambda}_{i,j} = \begin{cases} f & \text{for } j = i + s \\ 0 & \text{otherwise} \end{cases}. \tag{A4}$$

We assumed a constant per-capita death rate of 1, such that $d(i) = i$. The birth rate at population size i is $\beta_q \cdot i^2 + \beta_l \cdot i$, where $\beta_q \geq 0$ and $\beta_l \geq 0$ quantify the birth rates due to

processes that, respectively, do or do not require interactions such as cooperation or mate finding for reproduction. With different choices of the two parameters, this model produces a range of different scenarios. Scenarios B, C, and E in Fig. 1 are three such examples (See Table A1 for the corresponding parameter values). For $\beta_q > 0$, the birth rate is positively density-dependent. If, at the same time, $\beta_l + \beta_q < 1$, the birth rate is smaller than the death rate at small population sizes. Hence, the population experiences a strong demographic Allee effect with critical population size $(1 - \beta_l)/\beta_q$. Below this critical size, the population tends to decline and for small propagule sizes we thus obtain an ecological scenario with a difficult initial stage (Scenario B in Fig. 1). If, on the other hand, $\beta_q > 0$ and also $\beta_l + \beta_q > 1$, the population is expected to grow even at small sizes but its per-capita growth rate increases with population size. This so-called weak Allee effect is an easy scenario (scenario C in Fig. 1). If $\beta_q = 0$ and $\beta_l > 1$, the population grows exponentially (scenario E in Fig. 1).

Competition model

This model is a modified version of the competition model in Wittmann et al. (2013) and also has parallels to the model by Duncan and Forsyth (2006). The competition model is characterized by the fixed total community size K, the fecundity of the alien species relative to the native species w, and by the competition coefficient α, which specifies the strength of interspecific competition relative to intraspecific competition. Thus, the competition experienced by an individual whose own species has size x is $c(x, y) = x + \alpha \cdot y$ if the other species has population size y. We assume that the rate at which individuals die is proportional to the competition they experience. A dead individual is immediately replaced by an individual drawn at random from a large offspring pool to which individuals contribute in proportion to their fecundity.

For consistency with Wittmann et al. (2013), here the state n of the Markov process represents the current number of native individuals in the population, thus

$n \in \{0, 1, \ldots, K\}$. The transition rates due to birth and death events are then:

$$\bar{\lambda}_{n,n+1} = \underbrace{\frac{c(K-n,n)\cdot(K-n)}{K}}_{\substack{\text{rate at which} \\ \text{members of the alien} \\ \text{species die}}} \cdot \underbrace{\frac{n}{(K-n)\cdot w + n}}_{\substack{\text{probability that a} \\ \text{native individual} \\ \text{gives birth}}} \text{ for } n < K \tag{A5}$$

and

$$\bar{\lambda}_{n,n-1} = \underbrace{\frac{c(n,K-n)\cdot n}{K}}_{\substack{\text{rate at which} \\ \text{native individuals die}}} \cdot \underbrace{\frac{(K-n)\cdot w}{(K-n)\cdot w + n}}_{\substack{\text{probability that an} \\ \text{alien individual} \\ \text{gives birth}}} \text{ for } n > 0 \tag{A6}$$

and $\bar{\lambda}_{n,m} = 0$ for $m \notin \{n-1, n+1\}$.

The introduction process here is the same as in the single-population scenario. However, after each introduction event, the number of individuals in the community is truncated to K by randomly removing s individuals in proportion to the competition they experience. Thus, transitions due to introduction events happen at rates

$$\hat{\lambda}_{n,n-k} = f \cdot H[k, n, K-n+s, s, c(n, K-n+s), c(K-n+s, n)] \text{ for } n-k \in \{0, 1, \ldots, K\}, \tag{A7}$$

where $H[k, n, K-n+s, s, c(n, K-n+s), c(K-n+s, n)]$ is the probability mass function of Wallenius' noncentral hypergeometric distribution (Fog, 2008), i.e. the probability that in a community with n native and $K-n+s$ alien individuals, k native individuals are selected to be killed when drawing s individuals without replacement, and where native individuals have weight $c(n, K-n+s)$ and alien individuals weight $c(K-n+s, n)$. We computed H using the package BiasedUrn (Fog, 2011) in R (R Development Core Team, 2011).

We used the competition model to create scenarios A, D, F, and G in Fig. 1. The underlying parameter values can be found in Table A1.

Table A1. Models and parameter values underlying the ecological scenarios considered in the main text (see Fig. 1)

Scenarios generated by the single-population model				
Scenario		density-independent birth rate β_l	density-dependent birth rate β_q	target population size R
B		0	0.05	50
C		1.05	0.004	50
E		2	0	50
Scenarios generated by the competition model				
Scenario	competition coefficient α	alien fecundity w	carrying capacity K	target population size R
A	1.2	1	100	50
D	1.2	1	100	100
F	0.68	1	100	100
G	0.68	1	100	50

Analysis

For each model, the total transition rate from state i to state j, $\lambda_{i,j}$, is the sum of the transition rate due to introduction events and the transition rate due to other events:

$$\lambda_{i,j} = \hat{\lambda}_{i,j} + \bar{\lambda}_{i,j} \text{ for } i \neq j \, . \tag{A8}$$

λ_i is the total rate at which the Markov process leaves state i. These transition rates can be organized into a rate matrix $\mathbf{\Lambda}$ whose diagonal entries are given by $\lambda_{i,i} = -\lambda_i$.

When computing the expected time to reach the target population size R, only transitions from states with alien population sizes smaller than the target population size are relevant. We denote this set of states J. For the competition scenario, $J = \{K - R + 1, \ldots, K\}$ and for the single-population scenario $J = \{0, 1, \ldots, R - 1\}$. Now, consider a realization of the Markov process that starts in a state $i \in J$. Then the time T_i to reach state R can be decomposed into the time until the Markov process first leaves state i and the remaining time. Taking expectations and using the Markov property, we obtain:

$$\mathbf{E}[T_i] = \frac{1}{\lambda_i} + \sum_{j \in J, j \neq i} \frac{\lambda_{i,j}}{\lambda_i} \cdot \mathbf{E}[T_j]. \tag{A9}$$

Note that we do not need to include summands for states outside J, because once the process leaves J it has reached the target and the remaining time is 0.

The system of linear equations that consists of one such equation for each $i \in J$ was solved numerically in R (R Development Core Team, 2011) for T_{i_0}, the expected time belonging to the initial state i_0 ($i_0 = 0$ in the single-population scenario and $i_0 = K$ in the competition scenario). This corresponds to solving the matrix equation $\tilde{\mathbf{\Lambda}}\,\mathbf{E}[T] = -\mathbf{1}$, where $\tilde{\mathbf{\Lambda}}$ is the matrix obtained by removing from $\mathbf{\Lambda}$ all rows and columns belonging to the states that are not in J. $\mathbf{E}[T]$ is a column vector of expected times and $\mathbf{1}$ is a column vector with a 1 in each element. The expected times to reach the target state for the seven scenarios considered in the main text and for a propagule size of 1 are shown in Table A2.

Table A2. Expected times to reach the target population size for a propagule size of 1. The relative expected times in Fig. 2 refer to these values.

scenario	expected time
A	72.0
B	586.2
C	11.0
D	118.4
E	3.5
F	11254.6
G	13.0

Relative difference in expected time to reach the target

In the following sections, we explore the continuous dependence of the results on the parameters of our two models. To be able to visualize the results, we summarized the relative effect of propagule size and frequency within one quantity. To this end, we first computed the expected time of interest $\mathbf{E}[T]$ with propagule size s and propagule frequency f, and then computed the corresponding expectation $\mathbf{E}[T^*]$ with propagule size $s+1$ and propagule frequency $f \cdot s/(s+1)$. We then defined the sensitivity to this perturbation, our desired single quantity, as

$$\Delta := \frac{\mathbf{E}[T^*] - \mathbf{E}[T]}{\mathbf{E}[T]}\,, \tag{A10}$$

i.e. as the relative difference between the two expected times.

Under the hypothesis that only the product of propagule size and propagule frequency matters, we would expect $\Delta = 0$. Negative values of Δ represent cases where the introduction regime with the larger propagule size led to a faster invasion, whereas for positive Δ invasion was faster for the scenario with the higher propagule frequency. In the remainder of the text, we will abbreviate these two outcomes by saying that propagule size or propagule frequency have a larger effect, respectively. In addition to providing relative differences in expected times, we also show the rank correlation coefficients as a function of the model parameters.

Appendix 3 Results in dependence on model parameters

Single-population model

In the single-population model, the sensitivity score Δ (see equation A10) decreases with decreasing density-dependent birth rate β_q, or increasing $1/\beta_q$ (Fig. A2). In other words, the more interactions between individuals are required to produce an offspring in a density-dependent manner, the larger is the effect of propagule size. Under a weak Allee effect, however, propagule frequency remained the component with the larger effect for all values of β_q. If the Allee effect is strong, on the other hand, propagule size has a larger effect than propagule frequency for all but the smallest critical population sizes (small values of $1/\beta_q$). The latter cases actually represent easy ecological scenarios because the propagule size is larger than the critical population size. For easy scenarios, propagule frequency had a larger effect when it was small, whereas for difficult scenarios, a decrease in propagule frequency increased the effect of propagule size even more.

With increasing intensity of the Allee effect (increasing $1/\beta_q$) the expected time to reach the target population size became more strongly correlated to propagule size, while the correlation to propagule frequency became weaker (Fig. A3). Interestingly, for the parameter combination in Fig. A3 a, which represents a strong Allee effect, each of the three measures of propagule pressure had the strongest correlation with expected time in

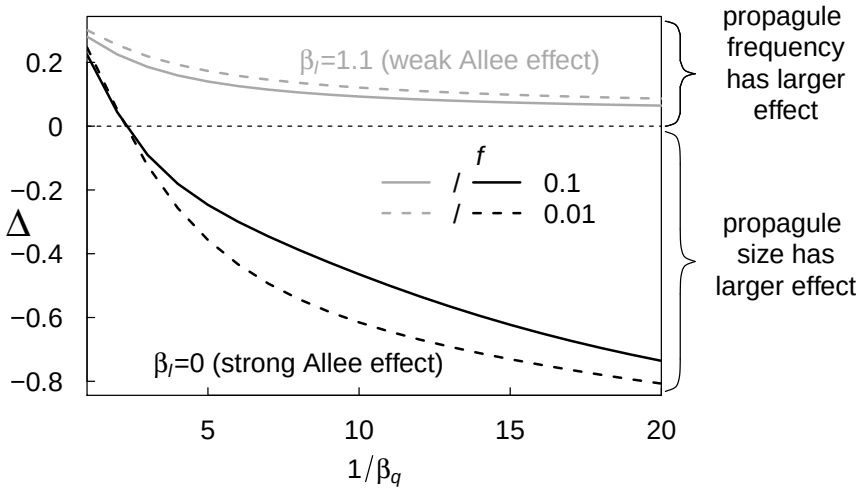

Figure A2. The sensitivity score Δ (see equation A10) as a function of the intensity of the Allee effect ($1/\beta_q$) in the single-population model with a strong ($\beta_l = 0$, black lines) or a weak Allee effect ($\beta_l = 1.1$, gray lines) and propagule frequencies f of 0.1 and 0.01. Note that with increasing values of $1/\beta_q$, the weak Allee-effect scenario approaches the exponential growth scenario. $R = 50, s = 3$.

some range of $1/\beta_q$: propagule frequency for very small values, i.e. small critical population sizes, the product for intermediate values, and propagule size for very high values, i.e. large critical population sizes. In the weak Allee effect scenario of Fig. A3 b, the measure with the strongest correlation to the expected times changed from propagule frequency to the product with increasing $1/\beta_q$, but over the parameter range we examined, propagule size always exhibited the weakest correlation.

Competition model

In the competition model, the sensitivity of expected times to perturbations in propagule size and frequency depends on the competition coefficient α and the alien species fecundity w (Fig. A4). In a symmetric competition situation ($w = 1$) with an advantage for the rare species ($\alpha < 1$), a high propagule frequency is more relevant for fast establishment, whereas a high propagule size helps the alien species to rapidly exclude the native species from the community. When the more common species has an advantage ($\alpha > 1$), propagule size has a larger effect for both establishment and exclusion of the native species. If $\alpha = 1$ and the alien species has a lower fecundity than the native species ($w < 1$), propagule size has a

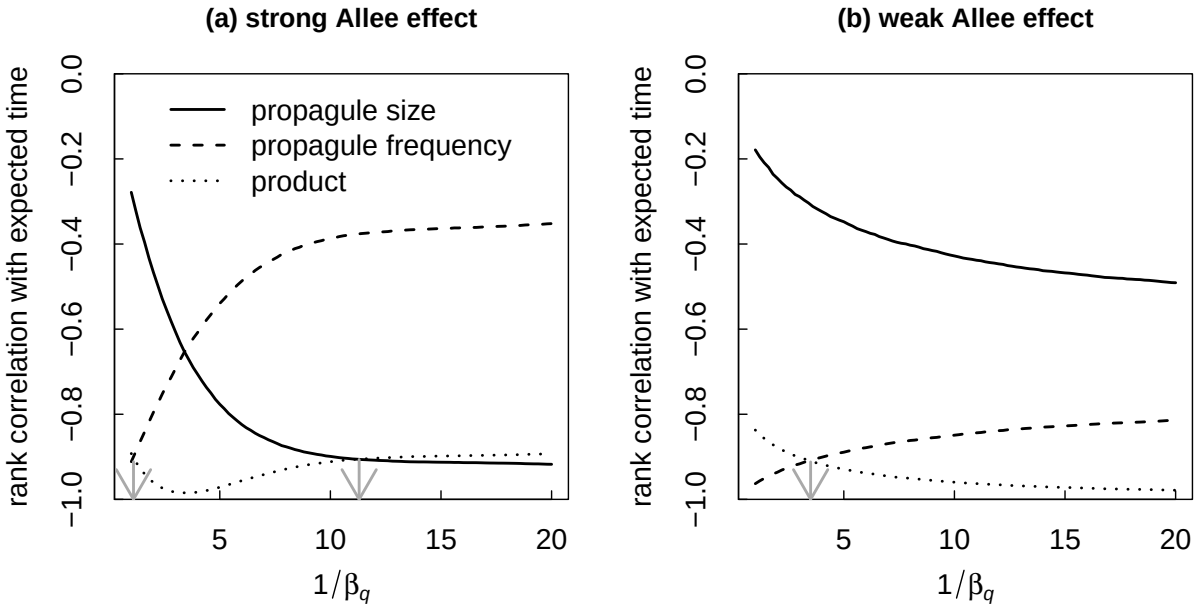

Figure A3. Rank correlation of the expected time to reach the target state and the three measures of propagule pressure as a function of the intensity of the Allee effect ($1/\beta_q$) in the single-population model. The strong Allee effect in (a) is produced by setting $\beta_l = 0$, whereas in (b) $\beta_l = 1.1$. The gray arrows indicate the points where a different measure of propagule pressure becomes the strongest correlator. The analysis is based on the introduction regime $(s, f) \in \{1, \ldots, 10\} \times \{0.005, 0.010, \ldots, 0.095, 0.1\}$. Note that with increasing values of $1/\beta_q$, the weak Allee-effect scenario approaches the exponential growth scenario. $R = 50$.

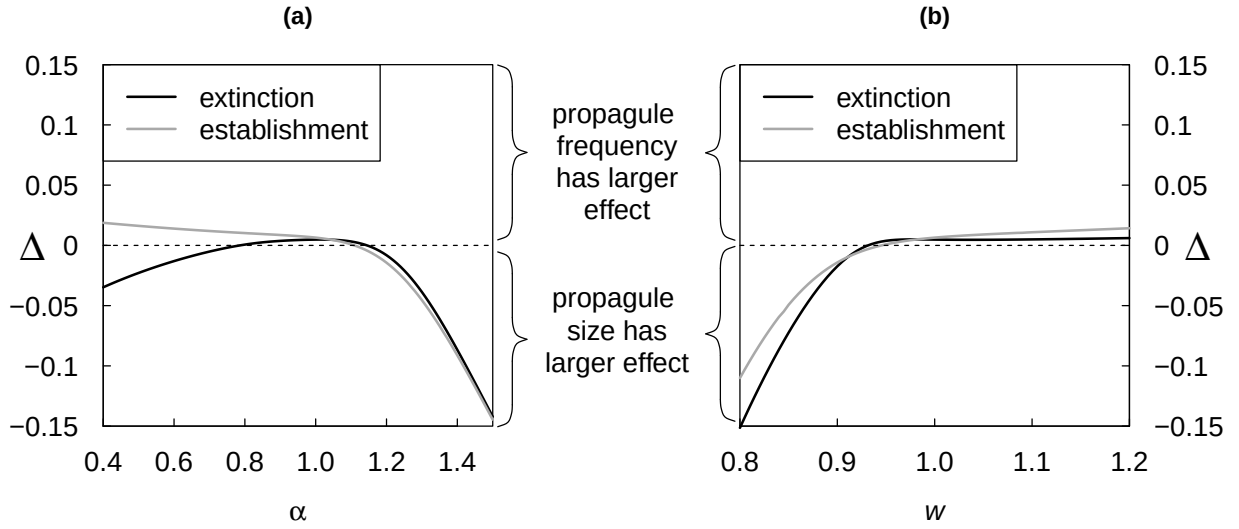

Figure A4. The sensitivity score Δ (see equation A10) of establishment time ($R = 50$) and native species extinction time ($R = 100$) in the competition model (a) for different competition coefficients α and (b) for different alien species fecundities w. $K = 100, f = 0.8, s = 3$. In a) $w = 1$; in b) $\alpha = 1$.

larger effect on both times of interest, whereas propagule frequency has a larger effect if the alien species has an advantage over the native species ($w > 1$). Other combinations of α and w are explored in Figs. A5 and A6.

According to the competition model, with the parameter combination examined in Fig. A7, the product always had the strongest correlation to the expected time to the extinction of the native species, whereas for the establishment time of the alien species, propagule frequency correlated more strongly for small competition coefficients. In general, the correlation coefficients for establishment time and extinction time behaved similarly for competition coefficients $\alpha > 1$, but diverged for $\alpha < 1$.

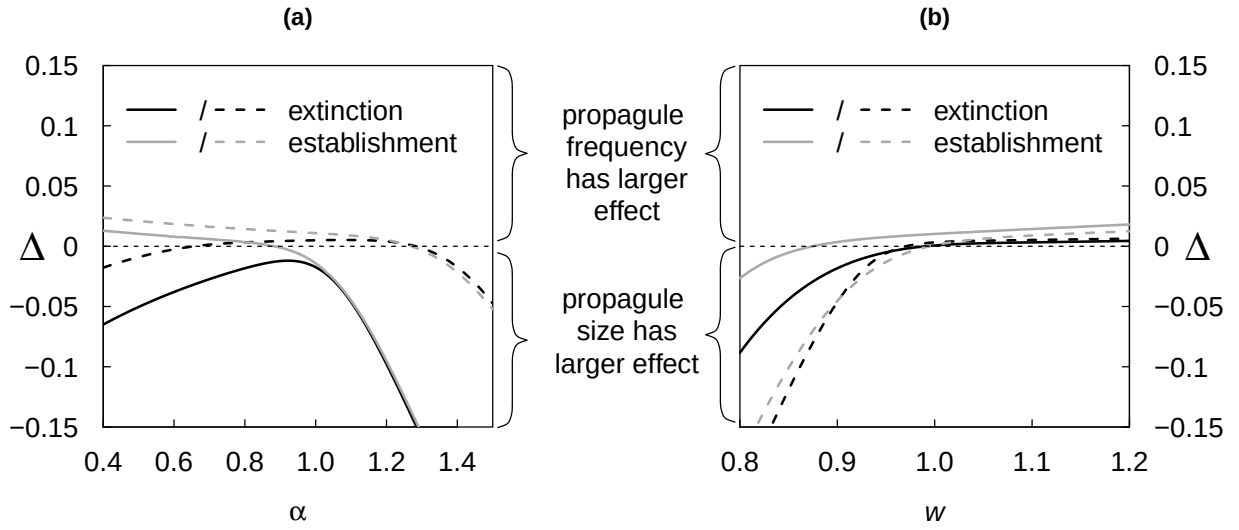

Figure A5. The sensitivity score Δ (see equation A10) of establishment time ($R = 50$) and native species extinction time ($R = 100$) in the competition model (a) for different competition coefficients α with $w = 0.9$ (solid lines) and $w = 1.1$ (dashed lines) and (b) for different alien species fecundities w with $\alpha = 0.8$ (solid lines) and $\alpha = 1.1$ (dashed lines). $K = 100, f = 0.8, s = 3$.

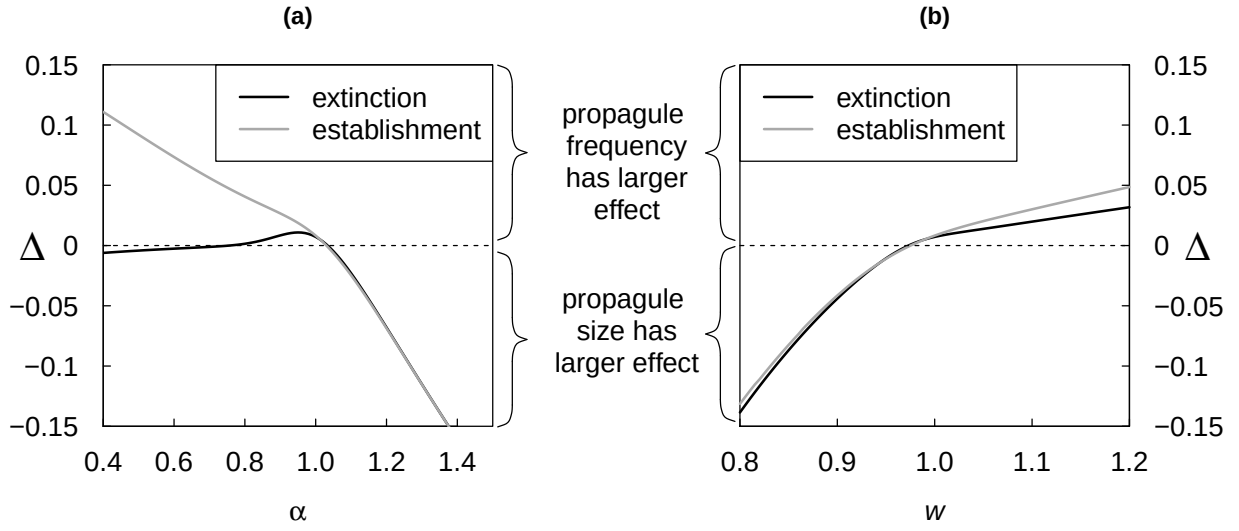

Figure A6. The sensitivity score Δ (see equation A10) of establishment time ($R = 50$) and native species extinction time ($R = 100$) in the competition model (a) for different competition coefficients α and (b) for different alien species fecundities w. The propagule frequency $f = 0.1$ is smaller than in Fig. A4. This leads to larger absolute values of Δ in the positive half-plane. $K = 100, s = 3$. In a) $w = 1$; in b) $\alpha = 1$.

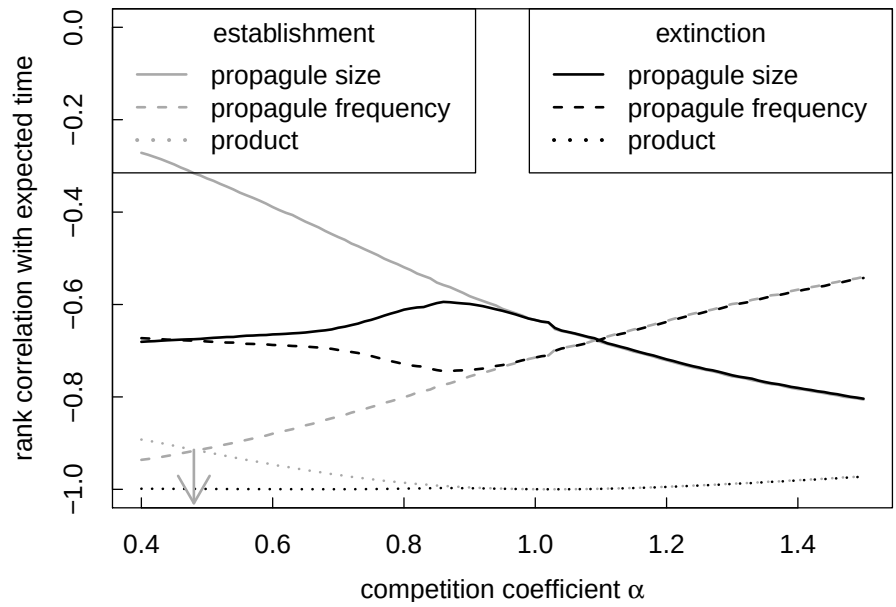

Figure A7. Rank correlation of the expected time to reach the target state ($R = 50$ for establishment and $R = 100$ for native species extinction) and the three measures of propagule pressure in the competition model for different competition coefficients α. The gray arrows indicate the points where a different measure of propagule pressure becomes the strongest correlator. The analysis is based on the introduction regimes $(s, f) \in \{1, \ldots, 10\} \times \{0.005, 0.010, \ldots, 0.095, 0.1\}$. $K = 100, w = 1$.

Appendix 4 Results for the single-population model with environmental change

Here we consider an extension of the single-population model in which there are two possible environmental states, 0 and 1, transitions between which happen at rate ϵ. The per-capita birth rates in environment 0 are $\beta_{l,0} = \beta_l \cdot \phi$ and $\beta_{q,0} = \beta_q \cdot \phi$. $\beta_{l,1} = \beta_l/\phi$ and $\beta_{q,1} = \beta_q/\phi$ are the corresponding rates in environment 1. Thus β_l and β_q are now the geometric averages of the birth rate parameters and $\phi \geq 1$ quantifies the magnitude of environmental change. With $\phi = 1$, the environment is constant and we get back to the original model. To summarize, in environment j and with a current population size of i, birth events happen at rate

$$b(i) = \beta_{l,j} \cdot i + \beta_{q,j} \cdot i^2 \,. \tag{A11}$$

To characterize the current state of the process, we now need two numbers: the population size i and the environmental state j. However, we can transform the model into

a one-dimensional Markov process with the help of a one-to-one map between the two-dimensional states and the natural numbers $\{1, \ldots, 2R\}$. After transformation, we can apply the same methods for its analysis as for the other models (described in Supplementary material Appendix 2). The results, corresponding to Figs. A2 and A3, are shown in Figs. A8 and A9. An increase in the magnitude of environmental change increases the sensitivity of expected times to propagule frequency. However, at least for the parameter combinations we considered, this effect is not strong enough to compensate the larger effect of propagule size under the difficult scenario of a strong Allee effect.

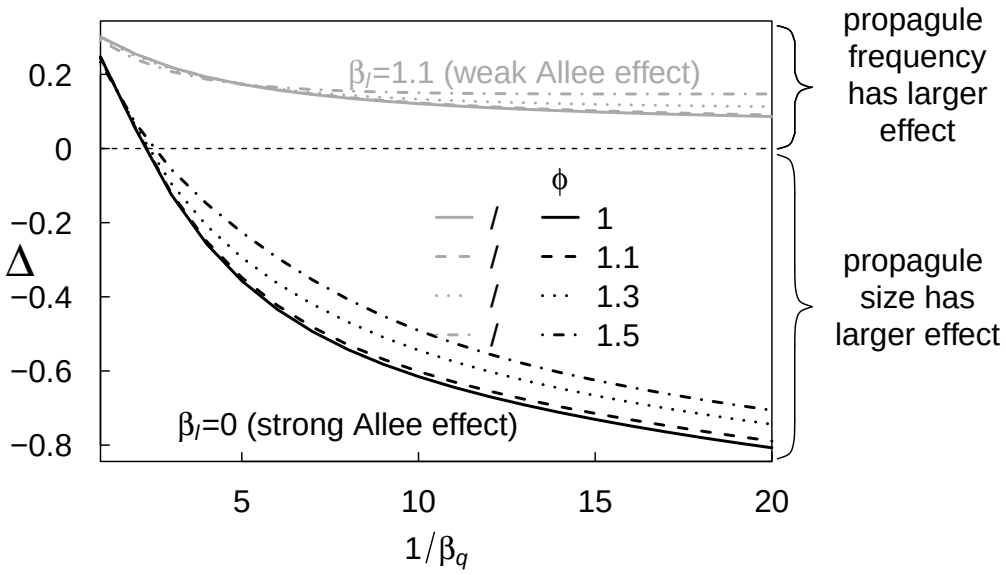

Figure A8. The sensitivity score Δ (see equation A10) as a function of the intensity of the Allee effect ($1/\beta_q$) in the single-population model with a strong ($\beta_l = 0$, black lines) or a weak Allee effect ($\beta_l = 1.1$, gray lines) and different magnitudes of environmental change ϕ. $R = 50, s = 3, f = 0.01, \epsilon = 0.1$, initial environment: 0.

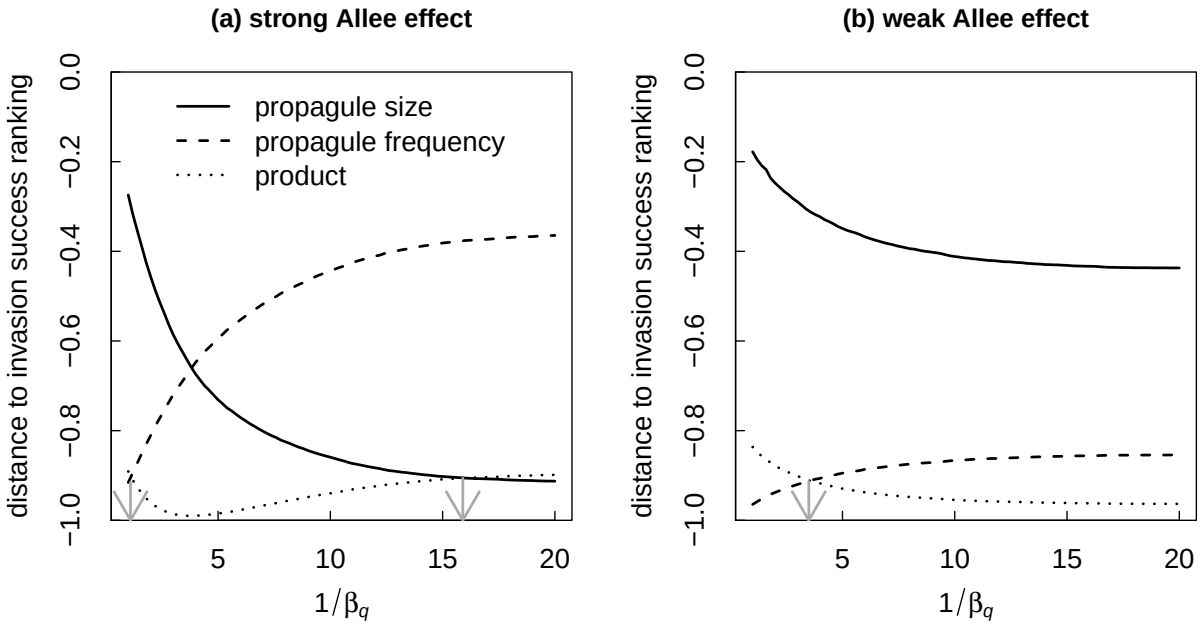

Figure A9. Rank correlation of the expected time to reach the target state and the three measures of propagule pressure as a function of the intensity of the Allee effect ($1/\beta_q$) in the single-population model with environmental change. The strong Allee effect in (a) is produced by setting $\beta_l = 0$, whereas in (b) $\beta_l = 1.1$. The gray arrows indicate the points where a different measure of propagule pressure becomes the strongest correlator. The analysis is based on the introduction regimes $(s, f) \in \{1, \ldots, 10\} \times \{0.005, 0.010, \ldots, 0.095, 0.1\}$. $R = 50, \phi = 1.5, \epsilon = 0.1$, initial environment: 0.

Appendix 5 Statistical models for the Australian dung beetle project

Here we provide details on the statistical analysis of the dung beetle data set from Tyndale-Biscoe (1996). Descriptive statistics for the seven species that we selected for our analysis are shown in Table A3. For each of the seven species, we fit logit-link binomial generalized linear models using the function glm (family "binomial") in R (R Development Core Team, 2011). The models were of the form

$$\log\left(\frac{p_i}{1-p_i}\right) = c_{intercept} + c_{size} \cdot s_i + c_{frequency} \cdot f_i + c_{product} \cdot s_i \cdot f_i, \qquad \text{(A12)}$$

where p_i is the success probability at location i, and s_i and f_i are the corresponding values for propagule size and propagule frequency. $c_{intercept}$, c_{size}, $c_{frequency}$, and $c_{product}$ are the

model coefficients. In each of the five candidate models, we set some of these coefficients to zero while estimating the others. As criterion for model selection, we used AIC (Burnham and Anderson, 2002), i.e. $-2 \cdot \text{log-likelihood} + 2 \cdot (\text{number of parameters})$, as implemented in the R function AIC (see Table A4). The model coefficients for the selected model are given in Table A5.

Note that whenever a one-factor model is chosen according to AIC, as was the case for all but one species, a likelihood-ratio test comparing it to a model with an additional parameter would never reject the simpler model on a 5 % level. The converse does not necessarily hold, but in the case of *Euoniticellus africanus*, a likelihood ratio test comparing the model with product and size to the model including only the product would reject the latter ($p = 3.6 \cdot 10^{-5}$).

In the case of *Euoniticellus africanus*, we also tested whether the model including the product and propagule size as predictors fits significantly better than the model with only propagule frequency. Since the two models are not nested, we could not use a likelihood-ratio test. To evaluate the significance of the observed difference in AIC values between the two models, we therefore ran simulations in R (R Development Core Team, 2011). The model assumed under the null hypothesis was the propagule-frequency model as fit to the observed data for *Euoniticellus africanus* ($c_{intercept} = -7.9$, $c_{frequency} = 74.4$, $c_{size} = c_{product} = 0$). Using this model and the same values for propagule size and frequency as in the observed data set, we generated 10,000 invasion success data sets. For each of them, we fit the two competing models and recorded their AIC values. In 14 % of the simulations, the model with the product and propagule size as predictors had an AIC advantage at least as large as the observed advantage. Thus, we conclude that this AIC difference is not significant on a 5 % level and we cannot reject the hypothesis that propagule frequency is the only influencing factor (p-value 0.14).

Table A3. Descriptive statistics on the biological control introductions of seven species of dung beetles (data from Tyndale-Biscoe, 1996). $\overline{f}$, $\overline{s}$, and $\overline{f \cdot s}$ give the average across locations of propagule frequency, propagule size, and their product, respectively. sd(f), sd(s), and sd($f \cdot s$) are the corresponding standard deviations. $\overline{\text{sd}}(s)$ is the average across locations of the estimated standard deviation of release sizes within one location.

Species	$\overline{f}$	sd(f)	$\overline{s}$	sd(s)	$\overline{f \cdot s}$	sd($f \cdot s$)	$\overline{\text{sd}}(s)$
Onthophagus gazella	0.201	0.207	841.9	729.3	217.09	420.53	792.3
Onitis alexis	0.109	0.103	415.8	176.9	44.01	41.99	108.58
Onthophagus binodis	0.078	0.041	824.9	675.9	65.38	68.22	537.32
Euoniticellus intermedius	0.231	0.204	629.5	644.5	129.75	117.04	18.99
Onthophagus taurus	0.111	0.067	896.7	445	96.55	61.1	285.34
Euoniticellus africanus	0.088	0.057	512.7	308.4	44.5	38.37	11.79
Hister nomas	0.165	0.165	516.2	184.2	88.66	111.93	194.13

Table A4. AIC values for the different candidate binomial GLMs for the success of seven species of dung beetles. AIC values of the respective selected models are printed in bold face.

Species	product	frequency	size	product + frequency	product + size
Onthophagus gazella	**78.10**	88.38	119.49	80.04	79.50
Onitis alexis	**78.19**	82.51	94.82	80.10	80.17
Onthophagus binodis	89.70	**89.29**	89.87	89.77	91.27
Euoniticellus intermedius	**59.38**	61.03	75.98	60.33	61.18
Onthophagus taurus	**51.97**	52.11	52.07	53.75	53.97
Euoniticellus africanus	31.59	17.56	41.56	19.07	**16.52**
Hister nomas	**25.45**	26.85	35.97	26.91	27.35

Table A5. Coefficients of the selected binomial GLM (see equation A12) for the success of seven species of dung beetles. Missing entries indicate that the corresponding predictor was not part of the selected model.

Species	$c_{intercept}$	$c_{frequency}$	c_{size}	$c_{product}$
Onthophagus gazella	-2.65			0.047
Onitis alexis	-2.08			0.058
Onthophagus binodis	-1.65	19.6		
Euoniticellus intermedius	-0.96			0.022
Onthophagus taurus	-0.66			0.002
Euoniticellus africanus	-3.83		-0.013	0.219
Hister nomas	-2.84			0.048

References

Burnham, K. P. and Anderson, D. R. 2002. Model Selection and Multimodel Inference. A Practical Information-Theoretic Approach. – Springer, 2nd ed.

Duncan, R. P. and Forsyth, D. M. 2006. Competition and the assembly of introduced bird communities. – In: Cadotte, M. W. et al. (eds.), Conceptual ecology and invasion biology. Springer, chap. 18, pp. 405–421.

Fog, A. 2008. Calculation methods for Wallenius' noncentral hypergeometric distribution. – Communications in Statistics-Simulation and Computation 37: 258–273.

Fog, A. 2011. BiasedUrn: Biased Urn model distributions. – R package version 1.04.

R Development Core Team 2011. R: A Language and Environment for Statistical Computing. – R Foundation for Statistical Computing.

Tyndale-Biscoe, M. 1996. Australia's Introduced Dung Beetles, Original Releases and Redistributions. – Technical report. CSIRO, Division of Entomology.

Wittmann, M. J. et al. 2013. Ecological and genetic effects of introduced species on their native competitors. – Theor. Popul. Biol. 84: 25–35.